ADVANCES IN ATMOSPHERIC SCIENCES, VOL. 25, NO. 4, 2008, 680–691

A New Global Four-Dimensional Variational Ocean Data Assimilation System and Its Application

LIU Juan[1,2] (刘 娟), WANG Bin[*1,2] (王 斌), LIU Hailong[1] (刘海龙), and YU Yongqiang[1] (俞永强)

[1] *State Key Laboratory of Numerical Modeling for Atmospheric Sciences and Geophysical Fluid Dynamics, Institute of Atmospheric Physics, Chinese Academy of Sciences, Beijing* 100029

[2] *Graduate University of Chinese Academy of Sciences, Beijing* 100049

(Received 30 April 2007; revised 22 September 2007)

ABSTRACT

A four-dimensional variational data assimilation (4DVar) system of the LASG/IAP Climate Ocean Model, version 1.0 (LICOM1.0), named LICOM-3DVM, has been developed using the three-dimensional variational data assimilation of mapped observation (3DVM), a 4DVar method newly proposed in the past two years. Two experiments with 12-year model integrations were designed to validate it. One is the assimilation run, called ASSM, which incorporated the analyzed weekly sea surface temperature (SST) fields from Reynolds and Smith (OISST) between 1990 and 2001 once a week by the LICOM-3DVM. The other is the control run without any assimilation, named CTL. ASSM shows that the simulated temperatures of the upper ocean (above 50 meters), especially the SST of equatorial Pacific, coincide with the Tropic Atmosphere Ocean (TAO) mooring data, the World Ocean Atlas 2001 (WOA01) data and the Met Office Hadley Centre's sea ice and sea surface temperature (HadISST) data. It decreased the cold bias existing in CTL in the eastern Pacific and produced a Niño index that agrees with observation well. The validation results suggest that the LICOM-3DVM is able to effectively adjust the model results of the ocean temperature, although it's hard to correct the subsurface results and it even makes them worse in some areas due to the incorporation of only surface data. Future development of the LICOM-3DVM is to include subsurface *in situ* observations and satellite observations to further improve model simulations.

Key words: 3DVM, 4DVar, ocean data assimilation, LICOM, SST

DOI: 10.1007/s00376-008-0680-6

1. Introduction

The ocean plays an important role in seasonal, annual and long term climate changes, which is the key area in investigating the global climate variation, especially since the frequent burst of El Niño can impact local, regional and global climate variations to different extents. The sparseness and irregularly temporal and spatial distributions of ocean measurements, however, make it difficult to study oceanic and related climate issues. In the last 20 years, the ocean data assimilation combining the observational data and model results in an optimal way provides us a useful tool to understand the physical principles of the ocean, following the development and improvement of the ocean observation system.

Since the 1980s, scientists have made great efforts in ocean data assimilation. For example, Derber and Rosati (1989) developed a global four-dimensional ocean data assimilation system; Anderson et al. (1996) reviewed advances in application of data assimilation techniques to problems in physical oceanography such as the evolution of ocean mesoscale eddies in middle latitudes, the development of El Niño events in the tropical Pacific, and the evolution of ocean surface waves; Ji et al. (1995, 1996), Ji and Leetmaa (1997), and Ji et al. (2000) focused on the initialization of the tropical Pacific and the prediction of ENSO; Evensen and Leeuwen (1996, 2000), Evensen (1997), devoted a lot to ensemble Kalman filter and nonlinear dynamics; Fukumori et al. (1999) studied the feasibility of assimilating satellite altimetry data into a global ocean

*Corresponding author: WANG Bin, wab@lasg.iap.ac.cn

general circulation model; Stammer et al. (2002) estimated a three-dimensional oceanic state and found a useful first solution to the global time-dependent ocean state estimation problem; Zhu et al. (2006), Yan et al. (2004) and Han et al. (2004) developed a three-dimensional variational (3DVar) ocean data assimilation system which takes temperature-salinity (T-S) relation into consideration and estimates temperature and salinity profiles from surface dynamic height information. In the operational application of data assimilation, 3DVar is widely used in most operational meteorological centers around the world, such as the Met Office (Lorenc, 1997), Canadian Meteorological Centre (Gauthier et al., 1999), National Centers for Environmental Prediction (NCEP) for Global Ocean Data Assimilation System (Seo and Xue, 2005) and the Japan Meteorological Agency for the ENSO prediction by the coupled ocean-atmosphere General Circulation Model (JMA-CGCM02) (Bloom et al., 1996). Furthermore, the European Centre for Medium-Range Weather Forecasts (ECMWF) (Rabier et al., 2000; Mahfouf and Rabier, 2000; Klinker et al., 2000) and the Canadian Meteorological Centre have also updated their ocean data assimilation systems to 4DVar systems.

At present, the methods of ocean data assimilation include optimal interpolation (OI), 3DVar, 4DVar and filtering. 3DVar is a popular method in operational forecasts and scientific research because of its low computing cost. Due to the lack of model constraints in 3DVar, however, 4DVar has been paid more and more attention. The major difficulty for the wide application of 4DVar in operational centers and research institutes is its huge computing costs for calculating the gradient of the cost function with model constraints by the adjoint technique.

To avoid the limitations of the traditional 4DVar, Wang and Zhao (2005, 2006) proposed a new 4DVar approach—three-dimensional variational data assimilation of mapped observation (3DVM). Like the available 4DVar method, 3DVM produces an optimal initial condition (IC) consistent with the prediction model due to the inclusion of model constraints and best fitting into the observations in the assimilation window through the model solution trajectory. Different from the old 4DVar, 3DVM requires much less computing cost closer to that of 3DVar (Wang and Zhao, 2005, 2006). This is the reason why this method is named 3DVM. So far, 3DVM has been used successfully in the initialization of typhoons and has achieved significant effects that are timesaving and efficient (Wang and Zhao, 2005, 2006; Zhao et al., 2007). May 3DVM be applicable for ocean data assimilation? Will it avoid the limitations in the old ocean data assimilation methods? This is what we attempt to answer in this paper.

The outline of this paper is as follows: Section 2 briefly describes the new 4DVar data assimilation method—3DVM. Sections 3 and 4 describe the data assimilation scheme, experiment design, the ocean model and the data used in this paper. Section 5 further analyzes the experiment results. A brief summary and conclusions are presented in the final section 6.

2. A brief description of 3DVM

According to Wang and Zhao (2005, 2006), the cost function of the old 4DVar may be expressed in incremental form (after tangential linear approximation):

$$J(x_0') = (x_0')^{\mathrm{T}} \boldsymbol{B}_0^{-1} x_0' + \sum_{i=1}^{N} (L_{t_0 \to t_i} x_0' - y_i')^{\mathrm{T}} \boldsymbol{O}_i^{-1} (L_{t_0 \to t_i} x_0' - y_i') \,, \tag{1}$$

where, x_0' and y_i' are defined by

$$\begin{cases} x_0' = x_0 - x_{0,\mathrm{b}} \,, \\ y_i' = x_{i,\mathrm{obs}} - x_i \,, \end{cases}$$

$x_{0,\mathrm{b}}$ is the background field at t_0, $x_i = M_{t_0 \to t_i}(x_{0,\mathrm{b}}\tau)$ $(i = 1, 2, \ldots, N)$ and $x_{i,\mathrm{obs}}$ are model forecast and observation at t_i, respectively, $\boldsymbol{B}_0$ is the background error covariance matrix at t_0, $\boldsymbol{O}_i$ is the observational error covariance matrix at t_i, M is the forecast model and $M_{t_0 \to t_i}(x_{0,\mathrm{b}}, \tau)$ is a mapping from t_0 to t_i by the model integration starting from $x_{0,\mathrm{b}}$ with the time step τ. L is the tangential linear model of the prediction model M which is invertible. 3DVM revised the background penalty term in the cost function based on the old 4DVar and produced the optimal IC at the end of the assimilation window, in contrast to the IC at the beginning of the window in the old 4DVar. The cost function of 3DVM can be expressed as an equivalent form of Eq. (1):

$$\tilde{J}(\tilde{x}') = \tilde{J}(x_0') = (\tilde{x}')^{\mathrm{T}} \boldsymbol{B}_N^{-1} \tilde{x}' + \sum_{i=1}^{N} (L_{t_0 \to t_i} x_0' - y_i')^{\mathrm{T}} \boldsymbol{O}_i^{-1} \times (L_{t_0 \to t_i} x_0' - y_i') \,, \tag{2}$$

where x_0' is the increment at the beginning of the window and $\tilde{x}'$ at the end of the window. These two initial perturbations satisfy

$$\tilde{x}' = x - x_{N,\mathrm{b}} \approx L_{t_0 \to t_i} x_0' \,, \tag{3}$$

where x is at the end of the window.

The relationship between $\boldsymbol{B}_N$ and $\boldsymbol{B}_0$ is

$$\boldsymbol{B}_N = L_{t_0\to t_N}\boldsymbol{B}_0 L^{\mathrm{T}}_{t_0\to t_N} , \tag{4}$$

which shows that the background error covariance matrix of 3DVM is flow-dependent. In Wang and Zhao (2005, 2006), the observationat $x_{i,\mathrm{obs}}$ at t_i is mapped to the end of the window through model mapping and the mapped observation $x_{i,\mathrm{mo}}$ at t_N is then found, where $x_{i,\mathrm{mo}}$ satisfies

$$x_{i,\mathrm{mo}} = M_{t_i\to t_N}(x_{i,\mathrm{obs}},\tau) = M_{t_i\to t_N}(x_{i,\mathrm{obs}}) . \tag{5}$$

For simplicity, we can omit τ in Eq. (5), since the time step is a constant. After a series of strict deductions, a neat form of the 3DVM cost function at the end of the time window is obtained:

$$\begin{aligned}\tilde{J}(x) =&(x-x_{N,\mathrm{b}})^{\mathrm{T}}\boldsymbol{B}_N^{-1}(x-x_{N,\mathrm{b}})+\\ &\sum_{i=1}^{N}(x-x_{i,\mathrm{mo}})^{\mathrm{T}}\tilde{\boldsymbol{O}}_i^{-1}(x-x_{i,\mathrm{mo}}) ,\end{aligned} \tag{6}$$

where $\tilde{\boldsymbol{O}}_i = L_{t_i\to t_N}\boldsymbol{O}_i L^{\mathrm{T}}_{t_i\to t_N}$.

For the details of 3DVM, the papers by Wang and Zhao (2005, 2006) can be referred. Note that all these studies are under the assumption that all variables at the model degrees of freedom are measured like other theoretical studies on 4DVar.

3. 3DVM-Based data assimilation scheme

Based on 3DVM, we developed a 4DVar system on the LASG/IAP Climate system Ocean Model (LICOM) (Liu et al., 2004a). The assimilation time length is seven days with 0000 UTC on Monday as the beginning of the window and the same time 7 days later as the end of the window. For the moment, the observational data used in this study is only the weekly-mean SST of the OISST from 1990–2001. Therefore, it's a challenge to satisfy the assumption of 3DVM. In the following section, we will address how to deal with this challenge.

To simplify the discussion, the same weekly-mean OISST data are supposed to be the observations at 8 different time points with an equivalent interval of one day in the assimilation window (including the beginning and the end of the window). Not only will such a supposition keep the average of the 8 observations consistent with the original OISST data, but it will also make up for the sparseness of the observations. Moreover, to meet the requirement of the 3DVM supposition that all variables at the model degrees of freedom are measured at the observation time, the model integration constraint is used to spread the observation information from the sea surface to other model layers which includes the following steps:

(1) choose a time such as 0000 UTC on Monday;

(2) use the OISST data to replace the temperature on the first model level (12.5 m) with the wind stress unchanged;

(3) integrate a time step by the model;

(4) repeat the steps (2) and (3) until balance is reached.

We have done experiments to determine when the model integration reaches balance. The normals of the global temperature field are calculated and when it becomes stable, we say it reaches balance. Usually, it needs at most 240 step iterations to reach the balance. In this way, the temperature field $T_{0,\mathrm{obs}}$ is obtained with observation information on every layer. The temperatures with observation information $T_{i,\mathrm{obs}}(i = 1,2,3,\ldots,7)$ at other times can be calculated similarly or are just assumed to be $T_{0,\ \mathrm{obs}}$, i.e., $T_{i,\mathrm{obs}} = T_{0,\mathrm{obs}}(i = 1,2,3,\ldots,7)$ according to the above supposition. There are 8 time points $t_i(i = 0,1,2,\ldots,7)$ in the assimilation window with t_0 at the beginning and t_7 at the end. The prediction model is defined as $M_{(\mathrm{T})}$ which satisfies:

$$M_{(\mathrm{T})} = M_{(\mathrm{T})}(T,W) ,$$

where T is temperature, W represents other variables such as surface elevation, velocity and salinity, and subscript (T) means temperature. This shows $M_{(\mathrm{T})}$ is only the temperature part of M. $W_i(i = 0,1,2,\ldots,7)$ is marked to be the value of W at the time, $t_0,t_1,\ldots,t_7$. Here, T and W are considered differently in order to obtain Eq. (15) and Eq. (16) since we treat T and W differently in our assimilation, which can be seen from Eq. (11) to Eq. (16). Mapping $T_{0,\ \mathrm{obs}}$ from t_0 to t_7, a mapped observation at t_7 is produced:

$$T_{0,\mathrm{mo}} = M_{(\mathrm{T})t_0\to t_7}(T_{0,\mathrm{obs}},W_0) . \tag{7}$$

Likewise, the other 7 mapped observations at the end of the window, respectively from $t_1,\ldots,t_6$ and t_7, can be generated:

$$\begin{cases} T_{1,\mathrm{mo}} = M_{(\mathrm{T})t_1\to t_7}(T_{1,\mathrm{obs}},W_1), \\ \qquad\cdots\cdots\cdots\cdots \\ T_{6,\mathrm{mo}} = M_{(\mathrm{T})t_6\to t_7}(T_{6,\mathrm{obs}},W_6) , \\ T_{7,\mathrm{mo}} = T_{7,\mathrm{obs}} . \end{cases} \tag{8}$$

Finally, 8 mapped observations at the end of the window through the model integration constraint are obtained:

$$T_{i,\mathrm{mo}}(i = 0,1,2,\ldots,7) . \tag{9}$$

Actually, we don't really need to integrate the model respectively for 7 days, 6 days, ... and 1 day to produce $T_{0,\mathrm{mo}}, T_{1,\mathrm{mo}}, \ldots$ and $T_{7,\mathrm{mo}}$ in the 3DVM. Only one 7-day model integration is required to generate all the mapped observations. In fact, when the ocean model is integrated from t_0 to t_1, the temperature at t_1, marked $T_{1,\mathrm{s}}$, is simulated:

$$T_{1,\mathrm{s}} = M_{(\mathrm{T})t_0\to t_1}(T_{0,\mathrm{obs}}, W_0)\ . \tag{10}$$

Then, the model integration from t_1 to t_2 continues with a new IC:

$$T_1^* = (\boldsymbol{O}_0^{-1} + \boldsymbol{O}_1^{-1})^{-1}(\boldsymbol{O}_0^{-1}T_{1,s} + \boldsymbol{O}_1^{-1}T_{1,\mathrm{obs}}) \tag{11}$$

rather than with the original $T_{1,s}$, and the temperature at t_2 is produced:

$$T_{2,s} = M_{(\mathrm{T}),t_1\to t_2}(T_1^*, W_1)\ . \tag{12}$$

Similarly, continuing the model integration until the end of the window, a general formula to calculate the temperature and the new IC at $t_i (i = 1, 2, \ldots, 7)$ is deduced

$$\begin{cases} T_0^* = T_{0,\mathrm{obs}}\ , \\ T_{i,s} = M_{(\mathrm{T}),t_{i-1}\to t_i}(T_{i-1}^*, W_{i-1})\ , \\ T_i^* = \left(\sum\limits_{k=0}^{i}\boldsymbol{O}_k^{-1}\right)^{-1}\left[\left(\sum\limits_{k=0}^{i-1}\boldsymbol{O}_k^{-1}\right)T_{i,s} + \boldsymbol{O}_i^{-1}T_{i,\mathrm{obs}}\right]\ . \end{cases} \tag{13}$$

Using the approximate equality: $f(\alpha x+\beta y) \approx \alpha f(x)+\beta f(y)$, whose proof is provided in the appendix, it is not difficult to deduce that

$$T_7^* \approx \left(\sum_{i=0}^{7}\boldsymbol{O}_i^{-1}\right)^{-1}\sum_{i=0}^{7}\boldsymbol{O}_i^{-1}T_{i,\mathrm{mo}}\ . \tag{14}$$

If the 3DVM cost function of LICOM 1.0 is written as follows according to Eq. (6):

$$J(T) = (T - T_{\mathrm{b}})^{\mathrm{T}}\boldsymbol{B}_N^{-1}(T - T_{\mathrm{b}}) + \sum_{i=0}^{7}(T - T_{i,\mathrm{mo}})^{\mathrm{T}}\tilde{\boldsymbol{O}}_i^{-1}(T - T_{i,\mathrm{mo}})\ , \tag{15}$$

the solution to $\nabla_T J(T) = 0$ is easily reached as the following

$$\begin{aligned} T_a &= \left(\boldsymbol{B}_N^{-1} + \sum_{i=0}^{7}\tilde{\boldsymbol{O}}_i^{-1}\right)^{-1}\left(\boldsymbol{B}_N^{-1}T_{\mathrm{b}} + \sum_{i=0}^{7}\tilde{\boldsymbol{O}}_i^{-1}T_{i,\mathrm{mo}}\right) \\ &= \left(\boldsymbol{B}_N^{-1} + \sum_{i=0}^{7}\tilde{\boldsymbol{O}}_i^{-1}\right)^{-1}\left[\boldsymbol{B}_N^{-1}T_{\mathrm{b}} + \left(\sum_{i=0}^{7}\tilde{\boldsymbol{O}}_i^{-1}\right)T_7^*\right]\ , \end{aligned} \tag{16}$$

where T and T_{b} are respectively the IC and background of temperature at the end of the window, $\boldsymbol{B}_N = L_{t_0\to t_N}\boldsymbol{B}_0 L_{t_0\to t_N}^{\mathrm{T}}, \tilde{\boldsymbol{O}}_i = L_{t_i\to t_N}\boldsymbol{O}_i L_{t_i\to t_N}^{\mathrm{T}}$. Clearly, the suggestion that only one 7-day model integration is needed is proved.

The observational error covariance matrix $\boldsymbol{O}_i$ at t_i is defined by:

$$\boldsymbol{O}_i = \boldsymbol{o}_i\boldsymbol{o}_i^{\mathrm{T}}\ .$$

Then,

$$\tilde{\boldsymbol{O}}_i = (L_{t_i\to t_N}\boldsymbol{o}_i)(L_{t_i\to t_N}\boldsymbol{o}_i)^{\mathrm{T}} = \tilde{\boldsymbol{o}}_i\tilde{\boldsymbol{o}}_i^{\mathrm{T}}\ ,$$

where $\tilde{\boldsymbol{o}}_i = L_{t_i\to t_N}\boldsymbol{o}_i$. $\boldsymbol{o}_i$ is the observational root mean square error, $\tilde{\boldsymbol{o}}_i$ consists of some samples created by integrating the tangential linear model. Therefore, $\tilde{\boldsymbol{O}}_i$ can be found through $\tilde{\boldsymbol{o}}_i$. Then the adjoint model is avoided and only the transpose of matrix is needed. As described in Wang and Zhao (2005, 2006), the tangential linear operator $L_{t_0\to t_i}$ can be formulated as the following:

$$L_{t_0\to t_i} = I + \tau D[M_{t_0\to t_i}(x_{\mathrm{b}}^0, \tau)]\ ,$$

where I is the unit operator, $D[M_{t_0\to t_i}(x_{\mathrm{b}}^0, \tau)]$ is the tangent linear tendency operator with respect to the basic state. And the term $\tau D[M_{t_0\to t_i}(x_{\mathrm{b}}^0, \tau)]$ is very small when the time step τ is limited in some range and the assimilation window is not too long, i.e.,

$$\|\tau D[M_{t_0\to t_i}(x_{\mathrm{b}}^0, \tau)]\| \ll \|I\|$$

So $L_{t_0\to t_i}$ can be approximated to I. In our experiment, we assume:

$$\boldsymbol{B}_N = \boldsymbol{B}_0 = \boldsymbol{B},\ \ \tilde{\boldsymbol{O}}_i = \boldsymbol{O}_i = \boldsymbol{O}\ .$$

As a theoretical study, $\boldsymbol{B}$ and $\boldsymbol{O}_i$ here are all supposed to be diagonal. According to Behringer et al. (1998), matrix $\boldsymbol{B}$ can be calculated experientially using the following formula

$$\boldsymbol{B}(x, y, z) \sim a_v\frac{(dT/dz)^{1/2}}{[(dT/dz)^{1/2}]_{\max}}\ , \tag{17}$$

where $a_v = 1.3$. The OISST product consists of both SST data and its normalized error variance E. Thereby, the variance of the observation error can be formulated as

$$\boldsymbol{O}^2 = \boldsymbol{\sigma}_m^2\boldsymbol{E}\ , \tag{18}$$

where $\boldsymbol{O} = \boldsymbol{O}(x, y), \boldsymbol{\sigma}_m^2$ is the guess error variance which is afforded by R. W. Reynolds (2006, personal communication). Suppose the subsurface covariance matrix of mapped observation error as the following:

$$\boldsymbol{O}(x, y, z) = \boldsymbol{O}(x, y)\exp\left\{\frac{z^2}{H^2}\right\}\ , \tag{19}$$

where H is the depth from the surface to the bottom at the location (x, y), z is the depth from the surface to the point (x, y, z). According to the assumption:

$$T_{i,\mathrm{obs}} = T_{0,\mathrm{obs}} (i = 1, 2, 3, \ldots, 7) ,$$

we can set $\boldsymbol{O}_i = \boldsymbol{O} (i = 0, 1, 2, \ldots, 7)$. When the difference between the observation and the background satisfies:

$$\Delta T > 5^{\circ}\mathrm{C} ,$$

the variance matrix of observation error may be defined as:

$$\boldsymbol{O}(x, y, z)[1 + (|\Delta T| - 5)^2] . \qquad (20)$$

At last, Eq. (16) may be expressed as the following form:

$$T_a = (\boldsymbol{B}^{-1} + 8\boldsymbol{O}^{-1})^{-1} (\boldsymbol{B}^{-1} T_{\mathrm{b}} + 8\boldsymbol{O}^{-1} T_7^*) . \qquad (21)$$

Using the above assimilation scheme, the assimilation run is designed based on a 12-year integration from January 1990 to December 2001 to assimilate OISST data.

4. The ocean model and datasets

The LASG/IAP Climate System Ocean Model, version 1.0 (LICOM1.0) has two versions at present, one with a high resolution of $0.5^{\circ} \times 0.5^{\circ}$ and the other with a coarse resolution of $1^{\circ} \times 1^{\circ}$. In this study, we choose the $1^{\circ} \times 1^{\circ}$ version of LICOM 1.0 for both CTL and ASSM, which is a global model covering the open sea from 90°N to 79°S. There are 30 vertical levels with 20 concentrated in the top 1000 m of the ocean. This model can simulate temperature, salinity and velocity well, and can reproduce the basic climate characters reasonably (Zhang et al., 2003a,b; Liu et al., 2004a; Wu et al., 2005). Also, it has been widely used in many aspects of climate modeling during the recent years (Liu et al., 2005; Yu et al., 2004; Yu et al., 2007; Zheng and Yu, 2007). A more detailed description of the model can be referred to Liu et al. (2004a).

The model was driven by the external forcing fields including net shortwave radiation, non-shortwave flux, the coupling coefficient from OMIP (Frank, 2001) and the daily wind stress from ERA40. World Ocean Atlas (WOA98) (Levitus et al., 1998) was applied to relax SST and sea surface salinity (SSS) towards their climatology. The 12-year integration from January 1990 to December 2001, without any assimilation, is referred to as CTL.

The SST observations used in the assimilation run (name ASSM) are Reynolds OISST with $1^{\circ} \times 1^{\circ}$ resolution, derived from analyzing the *in situ* data from all ship and buoy observations available in National Meteorological Center (NMC) on the Global Telecommunication System (GTS) using OI (Reynolds and Smith, 1994). The ship data depend on shipping traffic and are most dense in the mid-latitude Northern Hemisphere while sparse in the Southern Hemisphere. The buoy data have been designed to fill in some areas with little ship data. The satellite observations are obtained from the Advanced Very High Resolution Radiometer (AVHRR) on the U.S. National Oceanic and Atmospheric Administration (NOAA) polar orbiting satellites. The data used to validate the LICOM-3DVM system are WOA01 (Conkright et al., 2002), TAO (Hayes et al., 1991; McPhaden, 1995) and HadISST (Rayner et al., 2003). TAO data are daily and mainly distributed to the tropical Pacific, between 30°N–30°S. HadISST is the monthly mean SST dataset built by the Met Office Hadley Centre with a resolution of $1^{\circ} \times 1^{\circ}$ (Rayner et al., 2003).

5. Experiment results

The control and assimilation runs were performed on LASG cluster Lenovo 1801. The values of the cost

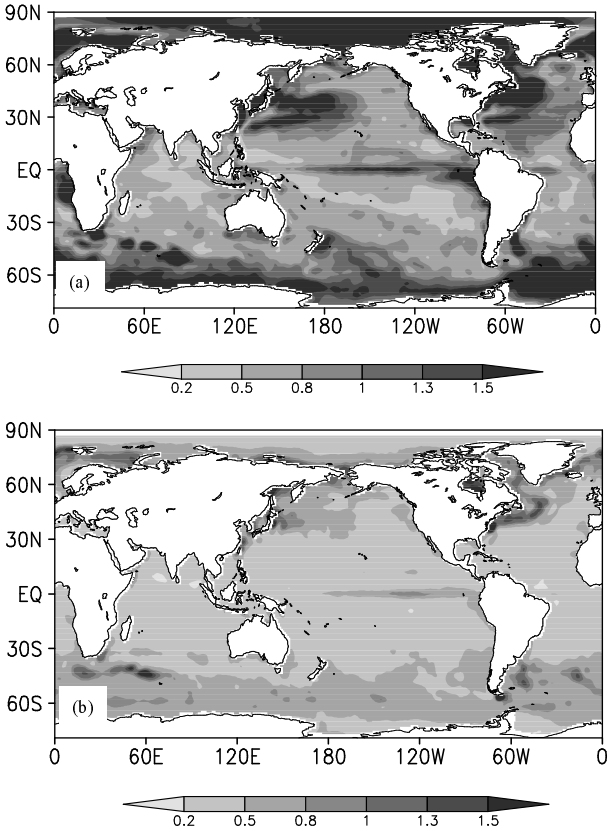

Fig. 1. RMSE of SST from (a) CTL and (b) ASSM, using the HadISST from January 1990–December 2001 as the true data. (Units: °C.)

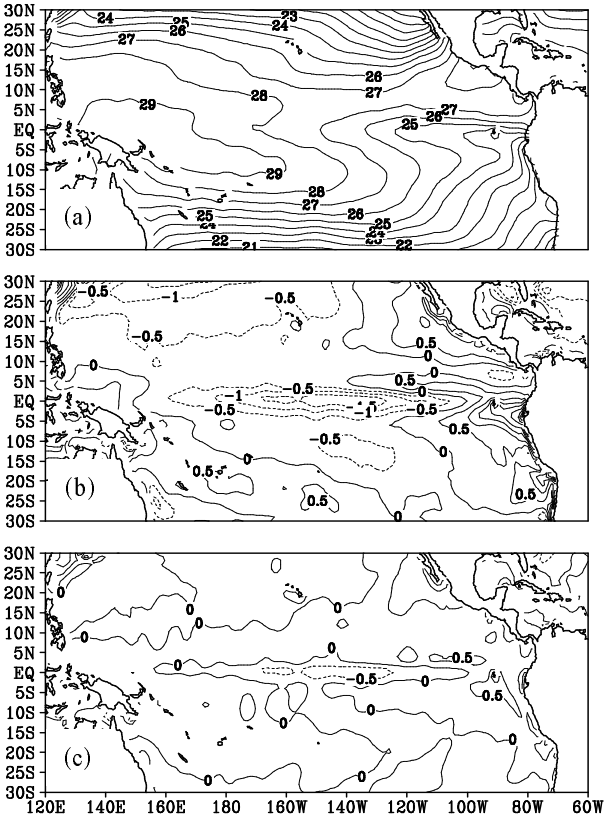

Fig. 2. Horizontal distributions of the 12-year averaged SST over tropical Pacific from (a) WOA01, (b) CTL minus WOA01, (c) ASSM minus WOA01. (Units: °C.)

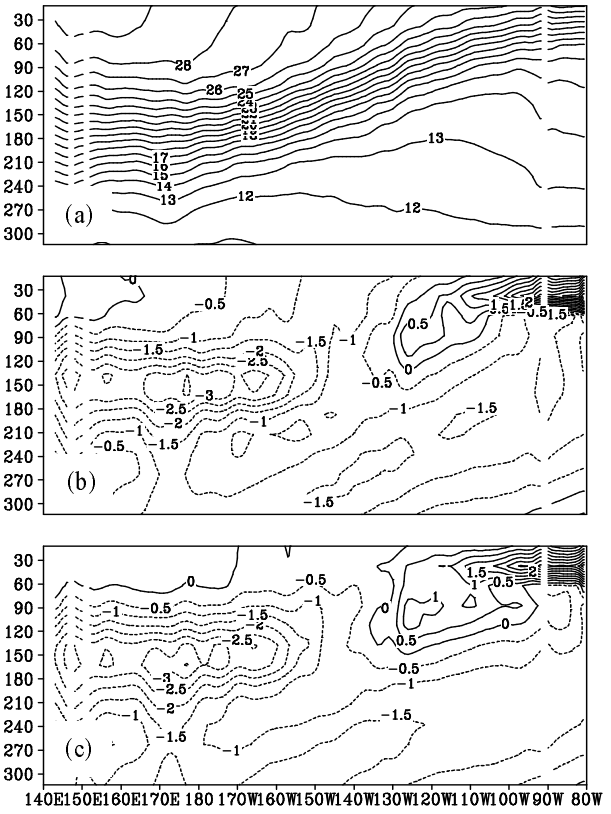

Fig. 3. The 12-year averaged temperature profile (averaged between 2°N and 2°S) from (a) WOA01, (b) CTL minus WOA01, (c) ASSM minus WOA01. (Units: °C.)

function which are the average of the 12-year experiment are respectively 1252090.1 before assimilation and 48454.9 after the assimilation. This indicates the success of ASSM in fitting the observation and demonstrates the efficiency of the LICOM-3DVM system in reducing the cost function. We will focus on the analysis and comparison of the temperatures, due to the only use of SST observation in the experiments.

The horizontal distributions of the root mean square errors (RMSEs) of the simulated SSTs from two experiments are calculated using the HadISST data as a reference, which are shown in Fig. 1. It is easily found that the RMSEs after assimilation are obviously less than those from CTL, especially in the regions where western boundary currents exist, such as the Kuroshio and the Gulf regions. The large RMSEs with the maximum value of 5°C in these regions from CTL are due to the narrow width of the regions, which are only 100 km wide and are hard for the ocean model to resolve horizontally. The use of 3DVM allows for significant improvement of the simulation in the regions. Also, the maximum RMSE in CTL is reduced to 10°C. As for the central and eastern Equatorial Pacific oceans, the RMSEs that reach 3°C and 2°C respectively in the control run are reduced to no more than 1°C after assimilation. Moreover, the globally averaged RMSE decreases from 1.082°C in CTL to 0.388°C in ASSM.

Consistent with the conclusion in Stockdale et al. (1998) that all ocean models have a cold bias in the equatorial upwelling region, the excessively-eastern-extension cold tongue with a 1°C cold bias is found in CTL (see Fig. 2) when comparing the 12-year averaged model SST over tropical Pacific with the WOA01 data. The result from ASSM eliminates the cold bias and coincides with the WOA01. In addition, the top-layer temperatures of CTL are much higher in the coast of South America while those from ASSM are closer to the observation.

From the 12-year averaged temperature profile (zonally averaged between 2°N and 2°S) in Fig. 3, we find that the main improvement occurs in the mixed layer, especially in the Equatorial central-eastern Pacific after assimilation. Beneath the mixed layer, however, little improvement is made by ASSM, compared with CTL. The most likely reason is that the subsurface temperatures in the tropical ocean are mainly affected by the upwelling and vertical mixing, but not

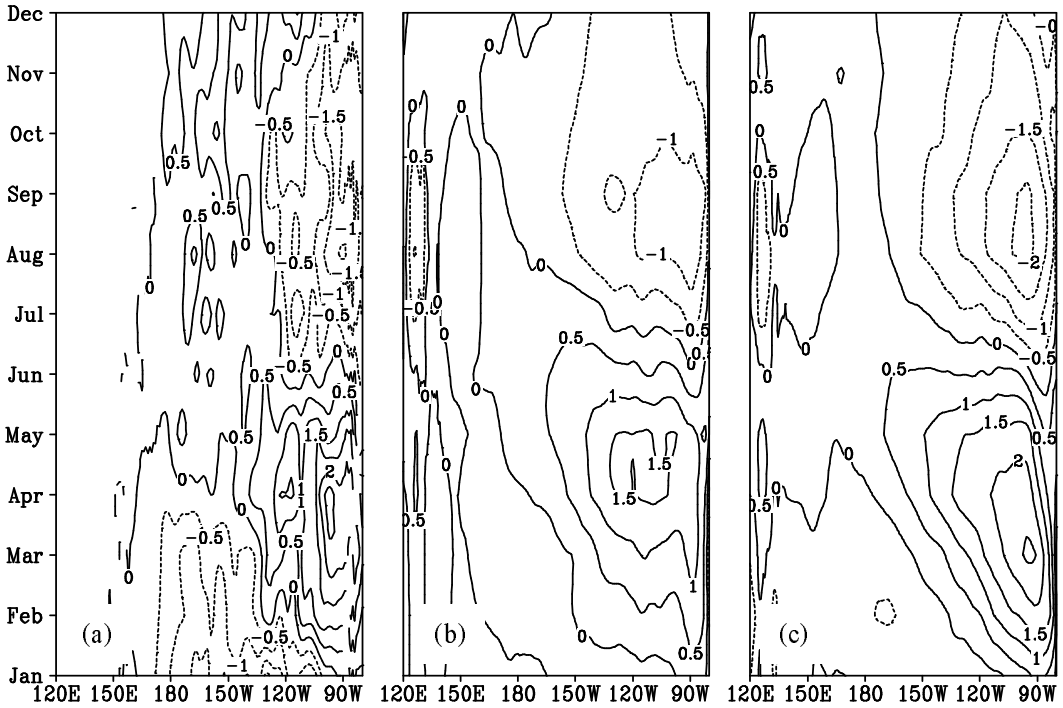

Fig. 4. The seasonal cycle of monthly SSTA (averaged between 2°N and 2°S) of (a) WOA01, (b) CTL, (c) ASSM. (Units: °C.)

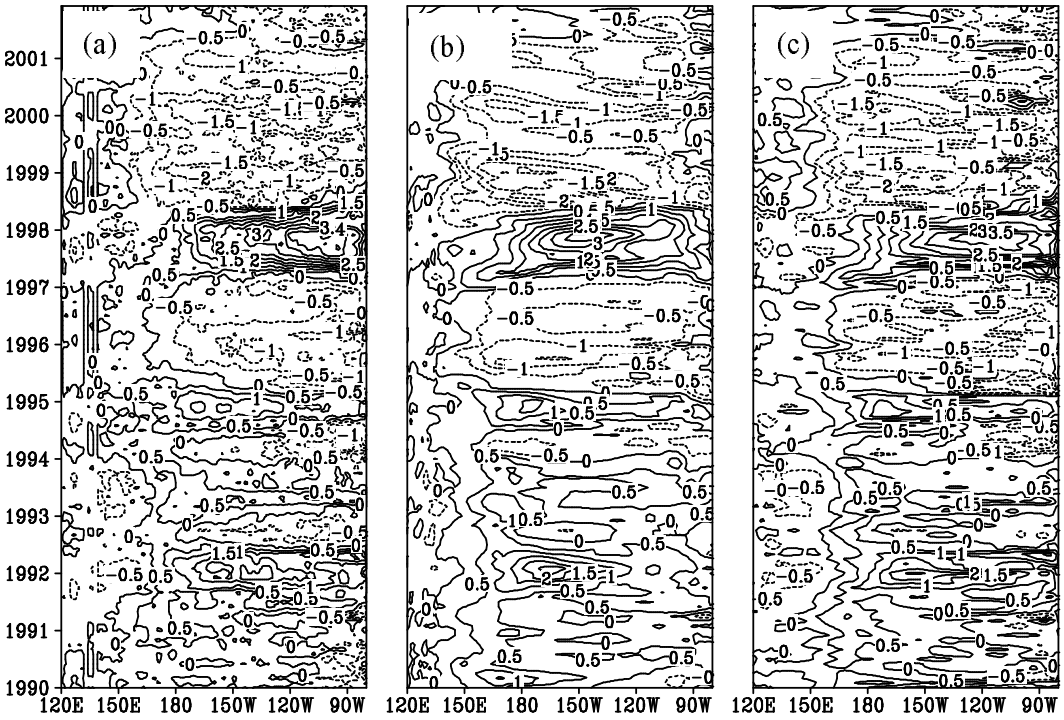

Fig. 5. Time-longitude plots of SSTA during 1990–2001 from (a) HadISST, (b) CTL, (c) ASSM (averaged between 2°N and 2°S). (Units: °C)

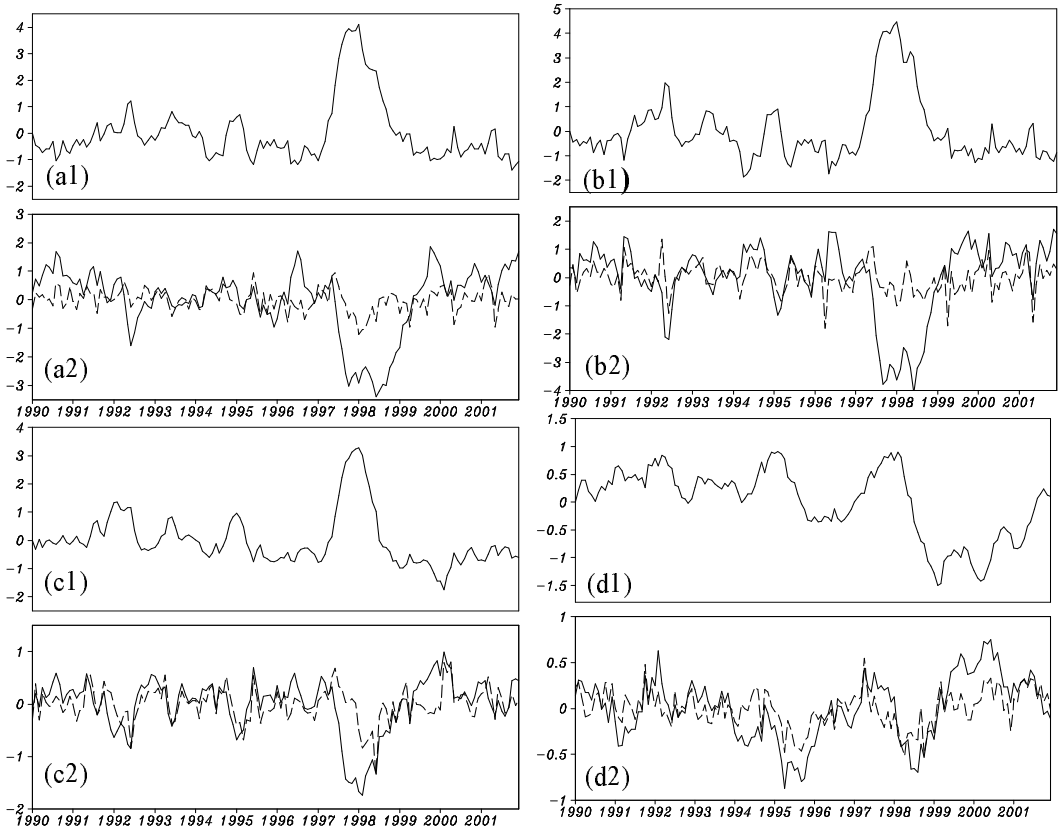

Fig. 6. The time series for (a1) and (a2) the Niño-1, (b1) and (b2) Niño-2, (c1) and (c2) Niño-3, and (d1) and (d2) Niño-4 SSTA and its differences between the model results and observations from January 1990 to December 2001. (a1), (b1), (c1) and (d1) are the time serials of observation, (a2), (b2), (c2) and (d2) are the differences between the model SSTA and that of HadISST for the CTL (the solid line) and the ASSM (the dashed line). Units: °C.

by SST due to the very small correlation between the SST and the subsurface temperature. The work of Zhu et al. (2002) confirms our results because the subsurface temperature in that study was not improved either after assimilating SST observations with an adaptive variational method. It was suggested in Zhu et al. (2002) that the temperature front at the bottom of the mixed layer is an obstacle for transmission of sea surface information to the subsurface. Tang and Kleeman (2004) analyzed the relationship between the temperatures at different levels and pointed out that the statistical relations between SST and subsurface temperature decay with the depth.

Plotted in Fig. 4 is the seasonal cycle of monthly SST anomaly (SSTA) (averaged between 2°N and 2°S). According to the WOA01, the SSTA is positive in spring due to the decreased trade winds and negative in autumn because of the strongly extended cold tongue in the eastern equatorial Pacific. The results of CTL, however, show a lower positive anomaly and a higher negative abnormality. Good agreements between ASSM and WOA01 can be seen clearly in Fig. 4.

Figure 5 shows the time-longitude distributions of SSTA averaged between 2°N and 2°S. While the cold and warm events described in CTL are of weaker strength, especially with the bias of −1.5°C in the strong 1997–98 El Niño event, the SSTA simulation from ASSM is good and is closer to the HadISST data.

The time series and the differences between the model results and observations for the Niño-1, Niño-2, Niño-3 and Niño-4 SSTA from January 1990 to December 2001 are shown in Fig. 6. Clearly, CTL fails to produce the Niño-1 and Niño-2 SSTA, which reveals a big model bias in these areas, though it's better for the Niño-3 and Niño-4 SSTA except at the peak. In contrast, ASSM provides good SSTA for all 4 Niño areas especially for the Niño events, compared with the HadISST.

After having analyzed the annual mean climatology, seasonal cycle and annual cycle of the temperature field above, the monthly averaged SST is taken into account. Compared with TAO data, the assimilation run successfully simulated SST in contrast with

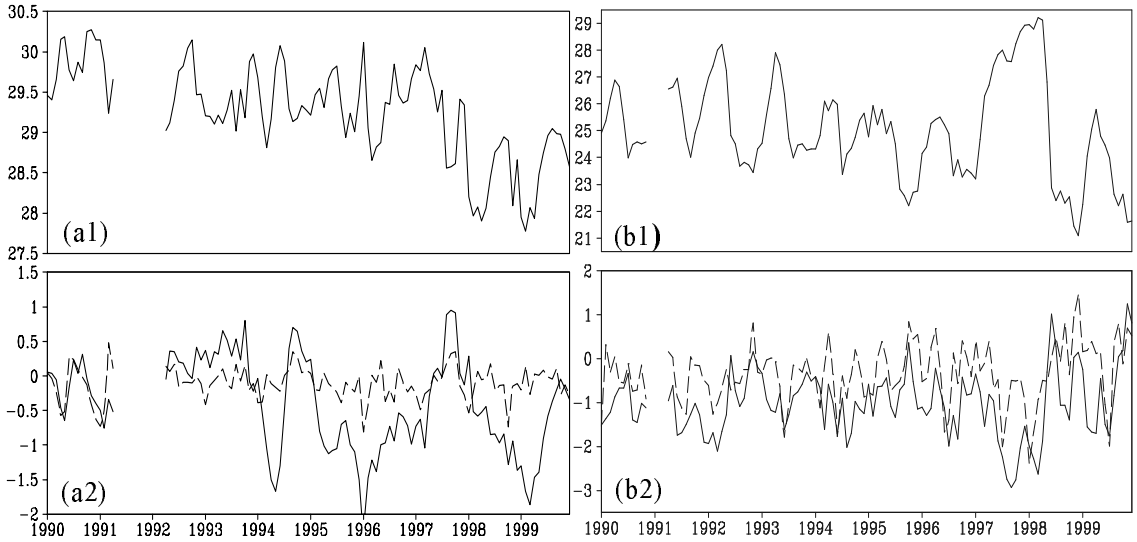

Fig. 7. The time series of monthly SST and the differences between the model SST and the TAO SST at point (a1), (a2), (2°N, 165°E), (b1), (b2), (0°N, 125°W). (a1) and (b1) are the time serials of TAO, (a2) and (b2) are the differences between the model SST and the TAO SST for the CTL (the solid line) and the ASSM (the dashed line). There are no observations from May 1991 to January 1992 for (2°N, 165°E) and from December 1990 to February 1991 for (0°N, 125°W). (Units: °C.)

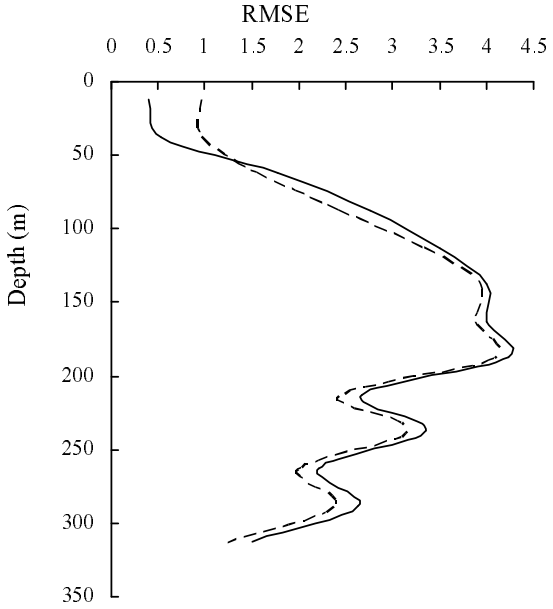

Fig. 8. The RMSE profile from ASSM (the solid line) and CTL (the dashed line), using the monthly TAO data during 1 January 1990–31 December 1999 as the truth. (Units: °C.)

CTL, which reveals good performance of the LICOM-3DVM system for SST simulation. This conclusion is supported by the results in Fig. 7, which gives the time series of SST and the differences between the model SST and the TAO SST for the CTL and the ASSM at points (0°N, 125°W) and (2°N, 165°E).

Figure 8 shows the RMSE profiles of the two experiments where TAO data from 1 January 1997 to 31 December 1999 are used as the observations. Compared with CTL, ASSM improved the temperature at the upper layers with the maximum depth of 50 meters by reducing the bias of 0.5°C, but did not improve the simulations below 50 meters.

The analysis above gives us a fact that ASSM is able to improve the simulations of temperature in the mixed layer. However, the univariate data assimilation of SST does not result in an improvement of other model variables, for example salinity and velocity field (Cooper, 1988; Masina et al., 2001). A comparison on the salinity between the two experiments shows no obvious differences are found (the figure is not given) since the variation of the salinity changes slowly. Also, the velocity field of ASSM shows no improvement when compared with the CTL (the figure is not given).

6. Conclusions

The main purpose of this paper is to apply a new 4DVar method—3DVM to the development and evaluation of an ocean data assimilation named LICOM-3DVM, based on the ocean model LICOM1.0. The model results can be improved through incorporating the weekly-mean OISST data into the model simulation by this new assimilation system.

Firstly, we gave an introduction of the 3DVM approach and formulated its implementation scheme ap-

plicable for the ocean data assimilation. The key point of 3DVM is to move the optimal initial condition of 4DVar from the beginning to the end of the assimilation window to avoid the adjoint technique for gradient calculation. A skill to map the observations at a different time up to the end of the window, newly proposed in this paper, highlights the efficiency of the 3DVM, which uses only one 7-day model integration to replace 7 model integrations with different time interval from 1 day to 7 day.

Secondly, the weekly OISST data were assimilated into the model simulations using the LICOM-3DVM system and the results were compared with those of CTL, the WOA01, the HadISST and the TAO data. The globally averaged RMSE of SST decreased from 1.082°C to 0.388°C after assimilation, which showed a good improvement in modeling SST. Great improvements on monthly-mean and annual-mean temperature in the mixed layer were also achieved by ASSM. It produced smaller cold bias of SST in the equatorial Pacific than CTL. Furthermore, the Niño SSTA coincides with the observation after assimilation. The experiment results strongly support the suggestion that the new 4DVar method—3DVM is effective for ocean data assimilation.

Due to the sparseness of observation, however, the improvements from ASSM occurred only at the upper layers such as the sea surface and the mixed layer. Further improvements of model simulations are required to incorporate more observed information, especially the subsurface data, which are underway.

Acknowledgements. The authors would like to thank Mr. R. W. Reynolds for providing the guess error variance of the OISST data. All computations of this work were completed on IAP1801 computer. This work was supported jointly by the Key Direction Project of the Chinese Academy of Sciences Knowledge Innovation Program (Grant No. KZCX-SW-230), the 973 Project (Grant No. 2005CB321703), and the National Natural Science Foundation of China (Grant No. 40221503).

APPENDIX A

The Proof of an Important Formula

Prove the formula below:

$$f(\alpha x+\beta y)-[\alpha f(x)+\beta(y)]=o(x-y)^2\ , \qquad \text{(A1)}$$

where f is a function, x, y, α and β are all real number, x and y are any variables, and α and β are constants satisfy $\alpha+\beta=1$.

Prove:

Suppose $\Delta x=y-x$, $s=\alpha x+\beta y$, then

$$s-x=\alpha x+\beta y-(\alpha+\beta)x=\beta(y-x)=\beta\Delta x\ , \qquad \text{(A2a)}$$

$$s=x+\beta\Delta x\ , \qquad \text{(A2b)}$$

$$s-y=\alpha x+\beta y-(\alpha+\beta)y=\alpha(x-y)=-\alpha\Delta x\ , \qquad \text{(A3a)}$$

$$s=y-\alpha\Delta x\ , \qquad \text{(A3b)}$$

$$f(s)=f(x+\beta\Delta x)=f(x)+\beta\Delta x f'(x)+o(\Delta x^2)\ , \qquad \text{(A4a)}$$

$$f(s)=f(y-\alpha\Delta x)=f(y)-\alpha\Delta x f'(y)+o(\Delta x^2)\ , \qquad \text{(A4b)}$$

$$f(s)=(\alpha+\beta)f(s)=\alpha f(s)+\beta f(s)= \alpha f(x)+\alpha\beta\Delta x f'(x)+\beta f(y)-\alpha\beta\Delta f'(y)\ , \qquad \text{(A4c)}$$

$$\begin{aligned} f(s)-[\alpha f(x)+\beta f(y)] &= f(\alpha x+\beta y)- [\alpha f(x)+\beta f(y)] \\ &= \alpha\beta\Delta x[f'(x)-f'(y)]+o(\Delta x)^2 \\ &= \alpha\beta\Delta x f''(x)(x-y)+o(\Delta x^2) \\ &= -\alpha\beta\Delta x^2 f''(x)+o(\Delta x^2) \\ &= o(\Delta x^2)\ , \end{aligned} \qquad \text{(A4d)}$$

$$\text{So}\quad f(\alpha x+\beta y)-[\alpha f(x)+\beta f(y)]=o(x-y)^2\ . \qquad \text{(A4e)}$$

When $o(x-y)^2$ is minor, the above equation can be written approximately as:

$$f(\alpha x+\beta y)=\alpha f(x)+\beta f(y)\ . \qquad \text{(A5)}$$

REFERENCES

Anderson, D. L. T., J. Sheinbaum, and K. Haines, 1996: Data assimilation in ocean models. *Reports on Progress in Physics*, **59**, 1209–1266.

Behringer, D. W., M. Ji, and A. Leetmaa, 1998: An improved coupled model for ENSO prediction and implications for ocean initialization. Part I: The ocean data assimilation system. *Mon. Wea. Rev.*, **126**, 1013–1021.

Bloom, S. C., L. L. Tacks, A. M. da Silva, and D. Ledvina, 1996: Data assimilation using incremental analysis updates. *Mon. Wea. Rev.*, **124**, 1256–1271.

Conkright, M. E., R. A. Locarnini, H. E. Garcia, T. D. O'Brien, T. P. Boyer, C. Stephens, and J. I. Antonov, 2002: World Ocean Atlas 2001: Objective Analyses, Data Statistics, and Figures, CD-ROM Documentation, National Oceanographic Data Center Internal Report 17, Silver Spring, MD, 17pp.

Cooper, N. S., 1988: The effect of salinity on tropical ocean models. *J. Phys. Oceanogr.*, **18**, 697–707.

Derber, J., and A. Rosati, 1989: A global oceanic data assimilation system. *J. Phys. Oceanogr.*, **19**, 1333–1347.

Evensen, G., 1997: Advanced data assimilation for strongly nonlinear dynamics. *Mon. Wea. Rev.*, **125**, 1342–1354.

Evensen, G., and P. J. V. Leeuwen, 1996: Assimilation of Geosat altimeter data for the Agulhas Current using the Ensemble Kalman Filter with a quasigeostrophic model. *Mon. Wea. Rev.*, **124**, 85–96.

Evensen, G., and P. J. V. Leeuwen, 2000: An Ensemble Kalman smoother for nonlinear dynamics. *Mon. Wea. Rev.*, **128**, 1852–1867.

Frank, R., 2001: An atlas of surface flues based on the ECMWF re-analysis—A climatological dataset to force global ocean general circulation models. Max-Planck-Insitut fur Meteorologie, Hamburg, Report No. 323, 31.

Fukumori, I., R., Raghunath, L.-L. Fu, and Y. Chao, 1999: Assimilation of TOPEX/POSEIDON altimeter data into a global ocean circulation model: How good are the results. *J. Geophys. Res.*, **104**(C11), 25647–25665.

Gauthier, P., C. Charette, L. Fillion, P. Koclas, and S. Laroche, 1999: Implementation of a 3D variational data assimilation system at the Canadian Meteorological Centre. Part I: The global analysis. *Atmos.-Ocean*, **37**, 103–156.

Han, G. J., J. Zhu, and G. Q. Zhou, 2004: Salinity estimation using the T-S relation in the context of variational data assimilation. *J. Geophys. Res.*, **109**, 1–12.

Hayes, S. P., L. J. Mangum, J. Picaut, A. Sumi, and K. Takeuchi, 1991: TOGA-TAO: A moored array for real-time measurements in the tropical Pacific Ocean. *Bull. Amer. Meteor. Soc.*, **72**, 339–347.

Ji, M., and A. Leetmaa, 1997: Impact of data assimilation on ocean initialization and El Niño prediction. *Mon. Wea. Rev.*, **125**, 742–753.

Ji, M., A. Leetma, and J. Derber, 1995: An ocean analysis system for seasonal to interannual climate studies. *Mon. Wea. Rev.*, **123**, 460–481.

Ji, M., A. Leetmaa, and V. E. Kousky, 1996: Coupled model forecasts of ENSO during the 1980s and 1990s at the National Meteorological Center. *J. Climate*, **9**, 3105–3120.

Ji, M., R. W. Reynolds, and D. W. Behringer, 2000: Use of TOPEX/Poseidon sea level data for ocean analyses and ENSO prediction: Some early results. *J. Climate*, **13**, 216–231.

Klinker, E., F. Rabier, G. Kelly, and J. F. Mahfouf, 2000: The ECMWF operational implementation of four-dimensional variational assimilation. Part III: Experimental results and diagnostics with operational configuration. *Quart. J. Roy. Meteor. Soc.*, **126 A**(564), 1191–1215.

Levitus, S., and Coauthors, 1998: Introduction. Vol. 1, *World Ocean Database 1998*. NOAA Atlas NESDIS 18, U.S. Government Printing Office, Washington, D.C., 346pp.

Liu, H. L., Y. Q. Yu, W. Li, and X. H. Zhang, 2004a: *Manual for LASG/IAP Climate System Ocean Model*, Science Press, Beijing, 107pp. (in Chinese)

Liu, H. L., X. H. Zhang, W. Li, Y. Q. Yu, and R. C. Yu, 2004b: An eddy-permitting oceanic general circulation model and its preliminary evaluations. *Adv. Atmos. Sci.*, **21**(5), 675–690.

Liu, H. L., W. Li, and X. H. Zhang, 2005: Climatology and variability of the Indonesian Throughflow in an eddy-permitting oceanic GCM. *Adv. Atmos. Sci.*, **22**, 496–508.

Lorenc, A. C., 1997: Develop of an operational variational assimilation scheme. *J. Meteor. Soc. Japan*, **75**(1B), 339–346.

Mahfouf, J. F., and F. Rabier, 2000: The ECMWF operational implementation of four-dimensional variational assimilation. Part II: Experimental results with simplified physics. *Quart. J. Roy. Meteor. Soc.*, **126A**(564), 1171–1190.

Masina, S., N. Pinardi, and A. Navarra, 2001: A global ocean temperature and altimeter data assimilation system for studies of climate variability. *Climate Dyn.*, **17**, 687–700.

McPhaden, M. J., 1995: The Tropical Atmosphere Ocean (TAO) Array is completed. *Bull. Amer. Meteor. Soc.*, **76**(5), 739–741.

Rabier, F., H. Jarvinen, E. Klinker, J. F. Mahfouf, and A. Simmons, 2000: The ECMWF operational implementation of four-dimensional variational assimilation. Part I: Experimental results with simplified physics. *Quart. J. Roy. Meteor. Soc.*, **126**, 1143–1170.

Rayner, N. A., and Coauthors, 2003: Global analyses of sea surface temperature, sea ice, and night marine air temperature since the late nineteenth century. *J. Geophys. Res.*, **108**(D14), 4407.

Reynolds, R. W., and T. M. Smith, 1994: Improved global sea surface temperature analyses using optimum interpolation. *J. Climate*, **7**, 929–948.

Seo, K. H., and Y. Xue, 2005: MJO-related oceanic Kelvin waves and the ENSO cycle: A study with the NCEP Global Ocean Data Assimilation System. *Geophys. Res. Lett.*, **32**, L07712,doi: 10.1029/2005GL022511.

Stammer, D., and Coauthors, 2002: Global ocean circulation during 1992–1997, estimated from ocean observations and a general circulation model. *J. Geophys. Res.*, **107**, C9, 3118–3144.

Stockdale, T. N., A. J. Busalacchi, D. E. Harrison, and R. Seager, 1998: Ocean modeling for ENSO. *J. Geophys. Res.*, **103**(C7), 14325–14355.

Tang, Y. M., and R. Kleeman, 2004: SST assimilation experiments in a tropical Pacific ocean model. *J. Phys. Oceanogr.*, **34**, 623–642.

Wang, B., and Y. Zhao, 2005: A new approach to data assimilation. *Acta Meteorologica Sinica*, **63**, 1–8. (in Chinese)

Wang, B., and Y. Zhao, 2006: A new approach to data assimilation. *Acta Meteorologica Sinica*, **20**(3), 275–282.

Wu, F. H., H. L. Liu, W. Li, and X. H. Zhang, 2005:

Effects of adjusting vertical resolution on the eastern equatorial Pacific cold tongue. *Acta Oceanologica Sinica*, **24**(3), 16–27.

Yan, C. X., J. Zhu, R. F. Li, and G. Q. Zhou, 2004: Roles of vertical correlations of background error and T-S relations in estimation of temperature and salinity profiles from sea surface dynamic height. *J. Geophys. Res.*, **109**, 1–18.

Yu, Y. Q., X. H. Zhang, Y. F. Guo, 2004: Global coupled ocean-atmosphere general circulation models in LASG/IAP. *Adv. Atmos. Sci.*, **21**, 444–455.

Yu, Y. Q., W. P. Zheng, H. L. Liu and X. H. Zhang, 2007: The LASG coupled climate model FGCM-1.0. *Chinese Journal of Geophysics*, **50**(6), 1677–1687. (in Chinese)

Zhao, Y., B. Wang, and Y. Q. Wang, 2007: Initialization and simulation of a landfalling typhoon using a variational bogus mapped data assimilation (BMDA). *Meteorology and Atmospheric Physics*, **98**, 269–282.

Zhang, X. H., Y. Q. Yu, and H. L. Liu, 2003a: The development and application of the oceanic general circulation models. Part I. The global oceanic general circulation models. *Chinese J. Atmos. Sci.*, **27**(4), 607–617. (in Chinese)

Zhang, X. H., Y. Q. Yu, R. C. Yu, H. L. Liu, T. J. Zhou, and W. Li, 2003b: Assessments of an OGCM and the relevant CGCM. Part I: annual mean simulations in the tropical Pacific ocean. *Chinese J. Atmos. Sci.*, **27**(6), 949–970. (in Chinese)

Zheng, W. P, and Y. Q. Yu, 2007: ENSO phase-locking in an ocean-atmosphere coupled model FGCM-1.0. *Adv. Atmos. Sci.*, **24**(5), 833–844, DOI: 10.1007/s00376-007-0833-z.

Zhu, J., H. Wang, and G. Q. Zhou, 2002: SST data assimilation experiments using an adaptive variational method. *Chinese Science Bulletin*, **47**(23), 2010–2013.

Zhu, J., G. Q. Zhou, C. X. Yan, W. W. Fu, and X. B. You, 2006: A three-dimensional variational ocean data assimilation system: Scheme and preliminary results. *Science in China* (*D*), **49**(11), 1212–1222.